XGEO Spacecraft Observation Methods Using Ground-Based Optical Telescopes

Kaitlyn Raub
The MITRE Corporation
Gregory Krzystyniak
The MITRE Corporation

ABSTRACT

The space industry is prospering – from the recent success of the first segment of the Artemis program to the upcoming Commercial Lunar Payload Services (CLPS) initiative preparing for nine excursions to the Moon. Consequently, it is imperative to adapt observation procedures used for spacecraft orbiting nearer to the Earth for the area of space beyond geosynchronous orbit (GEO), or XGEO. However, there are longstanding challenges surrounding XGEO, such as the complexity of the three-body problem and its subsequent orbits, as well as the difficulties in sensing objects many times more distant than GEO. These challenges render most traditional spacecraft tracking, detection, imaging, and observation generation techniques unusable.

This report details the findings from the research MITRE performed for ground-based optical observations of XGEO spacecraft. Included are the results of the MITRE XGEO collection campaign on more challenging targets, such as the James Webb Space Telescope (JWST), Artemis-1 Mission, and others. Discussed are the finalized telescope observing procedures used during the observation campaign on how to track, detect, and image targets over the span of XGEO space. Also included is information regarding updated data processing techniques to handle object correlation without the use of traditional methods, such as two-line element sets and standard propagation models, like SGP4.

1. INTRODUCTION

Humans are returning to the Moon for the first time in over 50 years starting with the Artemis missions, which aim to establish the first lunar base camp and orbiting lunar space station. The Commercial Lunar Payload Services (CLPS) program is slated to deliver nine landers to unexplored regions over the next five years and contain a variety of scientific instruments to study the environment of the Moon [1]. International parties are participating in this new era of lunar exploration as seen by prospective missions such as the Luna-25 lander from the Russian Space Agency destined for the south pole [2] and the Smart Lander for Investigating Moon (SLIM) from the Japanese Aerospace Exploration Agency (JAXA) which will demonstrate the ability for descent to the surface from low lunar orbit [3]. These missions only represent the beginning of what's to come for lunar exploration in the next decade.

Since spacecraft were initially placed in orbit around the Earth, objects within geosynchronous orbits (GEO) and nearer have taken immediate priority for ground-based space activities. With the increase of missions venturing further from the Earth's surface into XGEO space, the area beyond GEO, this extended region of space is quickly becoming an area of interest and concern.

Within XGEO space contains a sub-region called cislunar which refers to the volume of space where objects are traveling in proximity to the Moon. Objects in XGEO space exist beyond GEO while still being under the influence of Earth's gravity however spacecraft are not constrained to being physically near the Moon. While the distance to GEO is approximately 42,000 kilometers from the center of the Earth, XGEO is many times larger with objects reaching as far as 1,500,000 kilometers away. XGEO spacecraft are not only more distant in terms of linear distance but the volume of space which they can occupy is massive [4].

Approved for Public Release; Distribution Unlimited. Public Release Case Number 23-2669.

This creates a multitude of sensing and geometry challenges when attempting to track, detect, and image XGEO spacecraft using ground-based observatories with traditional observing methods. Optical sensors exhibit a sensitivity loss of $1/R^2$, where the brightness of light decreases by the inverse square of the distance. Distant spacecraft will be dimmer and more difficult to detect with our sensors. Given the angular resolution limitation of any sensor, these distances increase a sensor measurements cross-range uncertainty and make it more difficult to resolve closely spaced objects.

Additionally, XGEO objects have slow angular rates relative to our sensors due to these distances. Traditionally, satellites are tracked with the telescopes moving at the same rate of the target (i.e., rate tracking). This causes the satellite to remain stationary within images as a point source while background stars streak by. Observers can then distinguish between the streaking background of stars and the point source of light caused by objects traveling at or near the intended velocity of the target. With slow angular rates, the spacecraft and background stars within XGEO imagery all appear as point sources providing no visual indication for detection. Finally, cislunar objects are affected by the ”Cone of Shame”, an area of brightness illuminated by the reflected light from the Moon. This reflected light over saturates optical sensors and objects traveling in or near this volume of space are undetectable.

More challenges arise when looking at the astrodynamics of XGEO space. Unlike in nearer orbits, where Earth is the dominating gravitational force, XGEO objects interact strongly with not only the gravity from the Earth but also from the Moon and the Sun. This creates a more complicated gravity surface due to the interaction between the Earth, Moon, and Sun's gravity which changes the way spacecraft travel. For each pair of large bodies, such as the Sun-Earth or Earth-Moon system, 5 Lagrange equilibrium points form as shown in Fig. 1. Lagrange points are regions within a three-body system where the gravitational pull of two large bodies equals the centripetal force required for a smaller body to move within the system - effectively allowing an object to remain stationary [5].

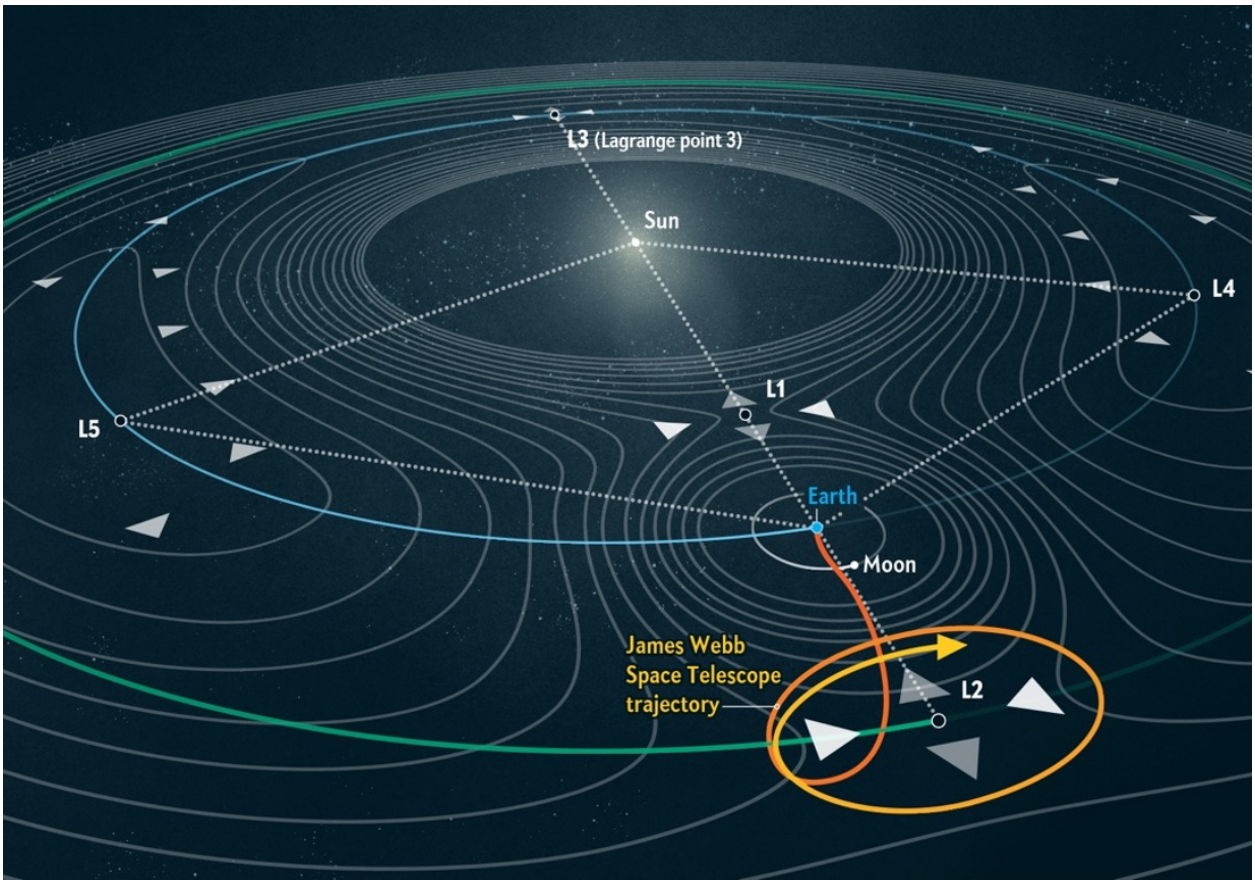

Fig. 1: The Lagrange diagram for a three-body system is shown. The contour lines represent changes in gravitational potential where more compact lines illustrate higher gravitational effects within the system. Objects within orbit close to any of the large bodies follow typical elliptical orbits while objects between the large bodies follow non-elliptical paths [5].

This system consists of five equilibrium points where three are unstable (L1, L2, L3) and two are stable (L4, L5). Coined as saddle points, the unstable points are regions where the potential curves upward in one direction and downward in another. A marble placed upon a horse saddle will move from their original position which is similar behavior to spacecraft placed within an unstable Lagrange point. While objects will require fuel expenditure to remain in orbit within a saddle point, they are strategic areas for certain missions such as Sun-Earth L1 being an ideal location to host solar observatories. The stable points, called hilltops, are regions where the potential is even so an object remains stationary with no fuel required to maintain orbit.

The interaction of three large bodies subsequently creates many orbit families that are chaotic, asymmetrical, and non-repeating for long periods of time as shown in Fig. 2. The Jet Propulsion Laboratory (JPL) has cataloged over 700,000 of these orbits to date [6].

Traditional methods for modeling the astrodynamics of spacecraft, such as the SGP4 propagation model, are not designed to handle the interactions of the three-body system, assume that Earth is the dominating gravitational force on the spacecraft, and treat the gravity of the Moon as a perturbation using low fidelity lunar gravitational models. Satellite orbits traditionally are described using two-line element sets (TLEs) which encode a list of orbital elements for Earth-orbiting objects. This modeling is not viable due to Earth no longer being the main gravitational influence on the XGEO spacecraft.

This report summarizes over two years of research spent developing an observation procedure for XGEO objects while investigating solutions to the sensing, geometry, and astrodynamic challenges described. While an initial observing procedure was explored in our previous paper for observing the James Webb Space Telescope [7], this report expands

on this by providing the results of the finalized XGEO observation procedure. We have tested our methods on a larger range of objects to include more difficult targets such as the Orion spacecraft from the Artemis-1 Mission and the GEOTAIL magnetosphere survey satellite. The resulting metric observation data is hosted within the Unified Data Library (UDL) as the first dedicated real-world data set of XGEO observations.

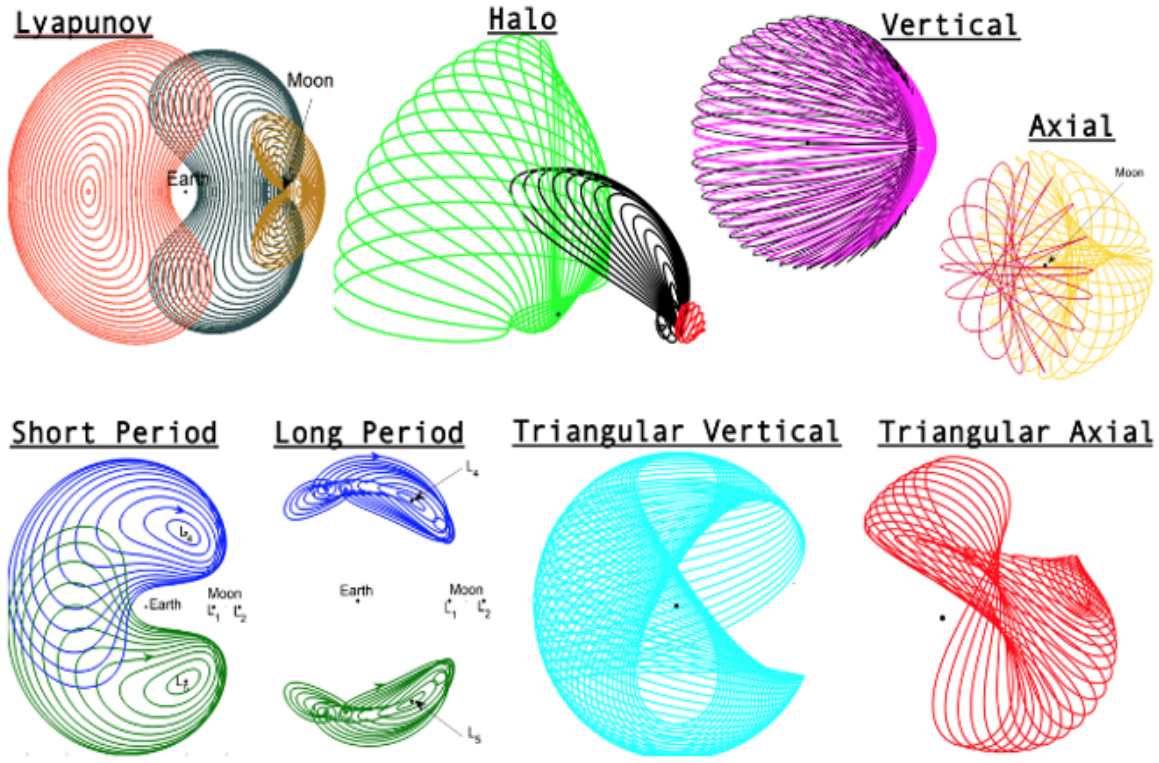

Fig. 2: Example of orbits created within a three-body system [6].

2. OBSERVING TARGETS

James Webb Space Telescope

Since its launch at the end of 2021, the James Webb Space Telescope (JWST) caught the attention of the world as the catalyst that propelled humanity into a new era of astronomy. Complete with 18 hexagonal segments that compose a massive 6.5-meter aperture primary mirror and a slew of sensors specializing in the infrared spectrum, the telescope is being tasked with answering some of humanities longest standing and most difficult astronomical questions.

The JWST has four primary objectives: to search for the first luminous objects formed after the Big Bang (i.e., "First Light"), to unravel the truth behind galactic evolution by observing the first galaxies formed to present day galaxies, to study the formation of stars and planets, and to measure chemical properties of planetary systems within our solar system and beyond in pursuit of finding the six main elements that are deemed fundamental for life (Sulfur, Phosphorous, Oxygen, Nitrogen, Carbon, and Hydrogen) [8].

The James Webb Space Telescope is currently hosted in orbit 1,500,000 kilometers from Earth within the Sun-Earth L2 point [9]. This orbit allows the JWST to meet the required cooling temperatures for the onboard sensors, with the cold side of the telescope housing the science instruments measuring at around -388° Fahrenheit [10].

Orion Spacecraft

The Artemis missions are how NASA plans to establish a human presence on and around the Moon through their Lunar Exploration Program [11]. The main objective of the Lunar Exploration Program is to provide facilities for astronauts to live and work while on lunar missions. The Artemis Base Camp will be constructed on the lunar surface

while Gateway will remain in orbit as the first lunar space station [12].

The Artemis program is broken down into segments with the first three completed or currently under development. The first segment (Artemis-1) served as the first test for not only the Orion Spacecraft, the space capsule that will carry astronauts from Earth to lunar orbit and back, but also the Space Launch System (SLS) Rocket, the only rocket that can send Orion, the astronauts, and cargo to the Moon on a single trip. The Orion Spacecraft and the SLS Rocket are the two key components for the entire success of the program. Artemis-1 launched at the end of 2022 successfully sending Orion to orbit about the Moon and safely returned to Earth around 25 days later.

GEOTAIL

As a joint project between JAXA and NASA, GEOTAIL was a survey satellite designed to study the structure and dynamics of the magnetosphere of the Earth. The spacecraft was launched in 1992 with its mission ending in November 2022 after 20 years of operation [13]. GEOTAIL resides in a highly elliptical orbit with a max distance of approximately 200,000 kilometers [14].

3. OBSERVATION PROCEDURE

Tracking

Due to two-line element sets being unusable for XGEO objects, we utilize ephemerides, a table of state vector information, for tracking. Ephemerides are generated through the JPL Horizons Service [15] which has updated models to appropriately handle the three-body system and accurate modeling of lunar gravitation and solar perturbations. Generating these state vector tables provides high fidelity tracking information for the telescopes and possess little accuracy degradation over time. This method does have limitations as there are currently no XGEO object catalogs available for generating ephemeris outside of Horizons. Although there are many objects available within Horizons, there are still targets outside of what JPL will publish ephemeris information for.

Imaging

To accommodate for the previously described sensing challenges associated with XGEO targets, we utilize longer exposure times and collection windows. While shorter exposure times (0.5-30 seconds) are adequate for nearer targets, XGEO objects require exposure times up to 120 seconds to provide enough sensitivity to be detectable within imagery. The telescope must also acquire long exposure images without external disturbances from the telescope mount or environmental effects like wind. Extended collection windows allow us to overcome the slow angular rate of XGEO objects by providing enough time between images for noticeable changes in the position of our targets to be seen. These collection windows, which originally were 15 minutes or less from start to finish, are now a minimum of 10 minutes between images for cislunar targets and 20 minutes for other XGEO objects.

Fig. 3. below shows the difference between images of XGEO objects compared to near-Earth orbiting objects. Using a 60-second exposure for the XGEO image, the JWST is a dim point source ambiguous among the background stars. The MEO image of NAVSAT 40105 uses a 0.5 second exposure which provides high signal of the target and the background stars are streaked which allows for immediate visual detection of the target.

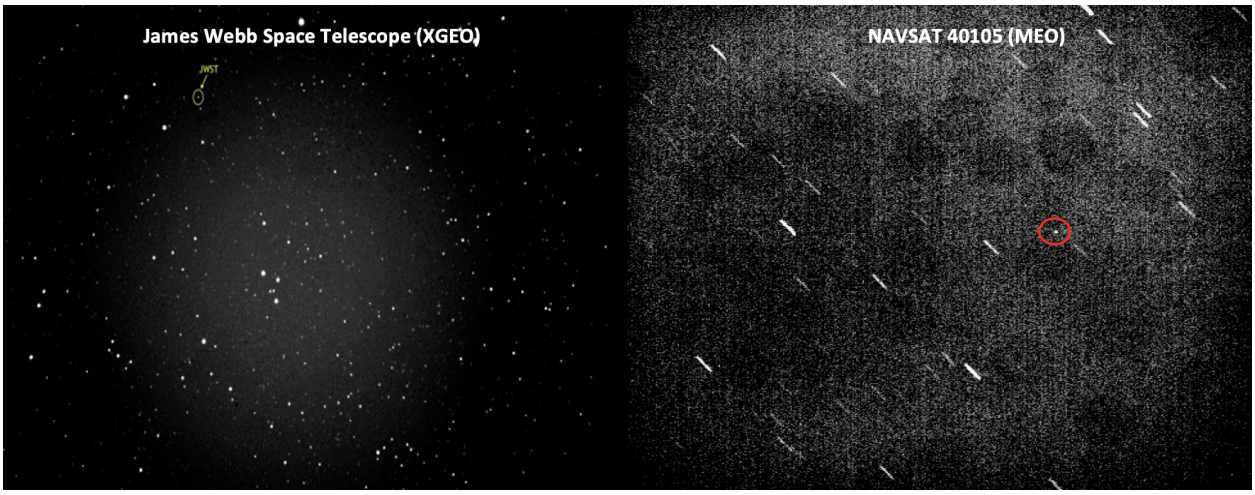

Fig. 3: Example imagery of an XGEO spacecraft (left) compared to a near-Earth spacecraft (right). The JWST image taken with a 60 second exposure provides low signal of our target and no streaking background stars for identification. The NAVSAT image taken with a 0.5-second exposure not only provides high signal of the target but has streaked background stars that immediately identify the satellite.

Detection

Due to the slow angular rate of XGEO objects relative to the sensors, an additional step was added to the observation procedure to handle identifying the target spacecraft. This is necessary for the image processing step as well as ensuring the telescope is tracking the correct area of space. This technique was inspired from asteroid detection methods [16] and is heavily used ranging from the Planetary Defense industry to citizen asteroid hunters. The method for detecting ambiguous spacecraft among background stars are:

1. Star-align the images using software to maintain the position of the background stars between frames.
2. Animate the images in chronological order by “blinking” the images as frames in a movie/GIF.
3. Locate any moving objects as the target.

Fig. 4. below demonstrates the outcome of this process.

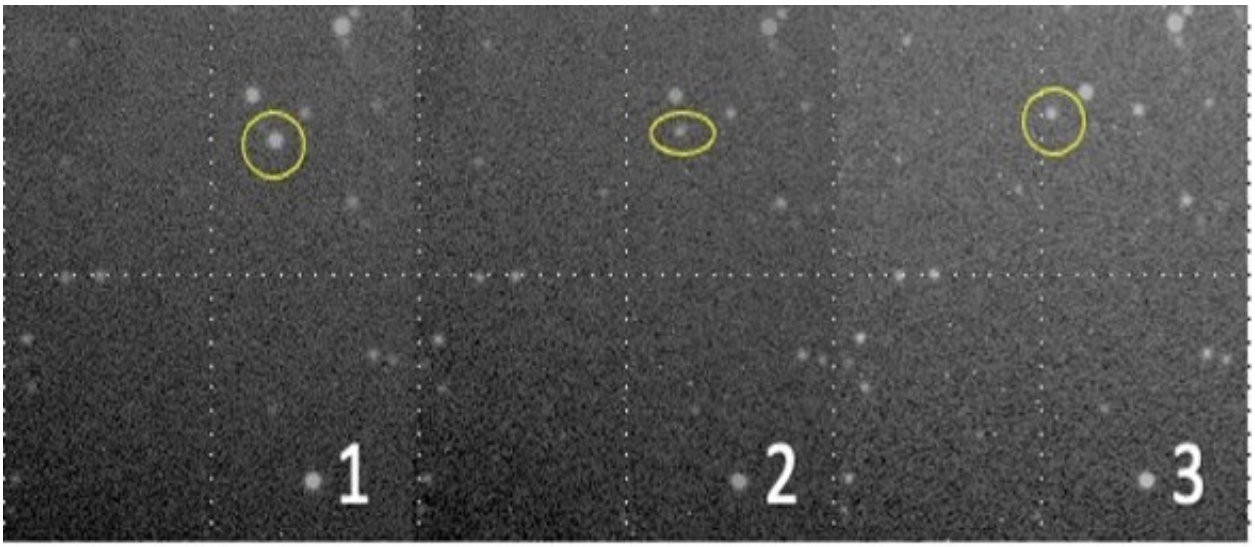

Fig. 4: Example of the effects of using the detection method to ”blink” images after star-aligning them. Non-stellar objects that are otherwise impossible to locate are now identifiable as they change in position. Looking at the numbered images in order, the circled object is seen moving to the left over time.

While this detection technique works well for bright objects, this process will be insufficient for dim targets or those that have minimal movement between images. An alternate detection technique was used for targets that fall into either of those categories which is:

1. Using the generated ephemeris, locate the state vector whose epoch matches the timestamp of the image.
2. Find the state vector RA and DEC within the image. If there is no object visible, the sensor was not able to detect the object.

This alternate method can be used in tandem with the detection technique to help locate the target especially for images with large fields of view or those with many background stars. Future work for increasing the efficiency of this detection method includes automating both of these procedures into one process that will find the target using the ephemeris then provide visual identification by marking where the target is located.

Image Processing

The image processing software natively uses a star catalog and a TLE catalog to perform object correlation and to produce metric observation data. The software also relies on streaking background stars to help distinguish between stars and spacecraft. Without TLE’s or streaking background stars, we implement a manual mode in the software which allows the user to select the target in each image to produce observation data. Future work for the image processing software includes adding the capability for ephemeris tables to be used for object correlation rather than only a TLE catalog. Additionally, if this ephemeris capability was added, there would be no need for the detection step discussed above as the image processing would handle target detection.

Table 1 below summarizes the differences in the procedure for observing XGEO spacecraft compared to observing GEO and nearer orbiting objects.

Table 1: Comparison of the MITRE observing procedure for near-Earth and XGEO objects.

Traditional Observing Procedure (LEO/GEO)	MITRE XGEO Observing Procedure
Short exposure times (0.5-5 seconds)	Long exposure times (30-120 seconds)
Short collection window (1-15 minutes)	Long collection window (30-180 minutes)
Object tracking using TLEs	Object tracking using ephemeris
Object detection using streaked background stars	Object detection using planetary defense method
Observation generation software utilizes TLE and star catalog	Observation generation software utilizes a manual mode to select the target object in each frame

4. OBSERVATION CAMPAIGN RESULTS

For the XGEO observation campaign, we tested our observing procedure on a handful of different targets. These spacecraft range from ones orbiting within the Sun-Earth L2 point to single month spacecraft missions venturing to the Moon and back. Aside from testing the observing procedure to successfully track, detect, and acquire imagery, the quality of the resulting metric observation data was evaluated and is described in this section. The complete set of observation data is available by request from active UDL users in the *MITRE Observations* and *MITRE Imagery* provider cards.

James Webb Space Telescope (SATID 50463)

The James Webb Space Telescope was first tracked during its launch in December 2021 with observations spanning through orbital insertion into its current host orbit of the Sun-Earth L2 point approximately 1,500,000 kilometers away. Table 2 summarizes the observing results for the JWST, including photometric and astrometric details, while Fig. 5. shows example imagery of the James Webb.

Table 2: Observation results for the James Webb Space Telescope.

Date	Mission Stage	Average Visual Magnitude	Average RA Error (Degrees)	Average DEC Error (Degrees)	# of Obs
December 27, 2021	Launch	12.60	0.0110	0.0060	104
January 5, 2022	Transfer Orbit	13.83	0.0059	0.0006	84
December 1, 2022	L2 Orbit	15.02	0.0052	0.0005	40
February 2, 2023	L2 Orbit	15.78	0.0053	0.0001	73
February 3, 2023	L2 Orbit	15.55	0.0050	0.0001	38
February 7, 2023	L2 Orbit	17.01	0.0051	0.0009	60
February 8, 2023	L2 Orbit	17.81	0.0053	0.0004	5
March 29, 2023	L2 Orbit	17.25	0.0059	0.0017	7
March 30, 2023	L2 Orbit	17.52	0.0058	0.0017	33

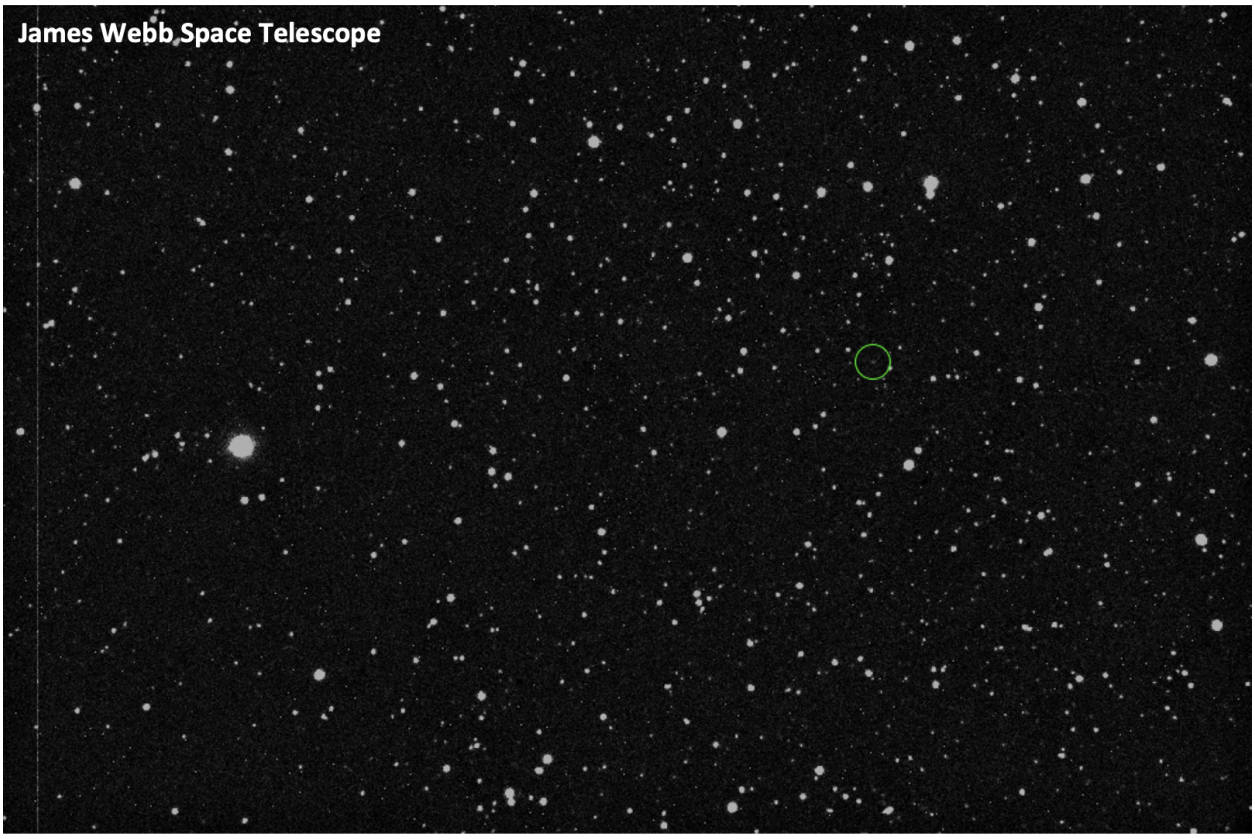

Fig. 5: Imagery of the James Webb Space Telescope taken with the MITRE Observatory on December 1, 2022, while the JWST was in Sun-Earth L2 orbit.

As shown previously [7], using data acquired from launch provided an opportunity to characterize changes in the visual magnitude of the James Webb to different stages of its mission. This includes observing changes in brightness of the JWST correlated to the sun shield being deployed or the primary mirror being assembled. Additionally, we show an example of how our observing procedure successfully extends to observing multiple objects simultaneously by detecting the rocket body that delivered the James Webb into space.

The James Webb Space Telescope is the furthest object successfully observed with our observatory at over 1,500,000 kilometers away. The JWST was best imaged using a sidereal tracking mode due to the slow angular rates of the target. Using a sidereal tracking mode allowed for increased fidelity when performing the star alignment in the detection step. For imaging, we found a 60-second exposure most successful. This exposure time allowed for enough photons to be collected by our sensors to detect the image but was short enough to not have interference from the environment. Despite being on its journey to Sun-Earth L2 or being stationed in the host orbit, the astrometric errors for right ascension (RA) or declination (DEC) were consistent between observations. As the most distant object observed, increased collection windows were used to have enough movement in the position of the target between images. A minimum of 20 minutes was required between images for any angular movement and we used a minimum of 60 minutes for the total collection window.

Orion (SATID 54257)

The Orion spacecraft was observed during its journey to lunar orbit and while returning to the Earth during the Artemis-1 mission at the end of 2022. The Orion spacecraft reached over 400,000 kilometers from Earth. Table 3 summarizes the observing results for the Orion spacecraft including photometric and astrometric details while Fig. 6. shows example imagery of the spacecraft.

Table 3: Observation results for the Orion spacecraft.

Date	Mission Stage	Average Visual Magnitude	Average RA Error (Degrees)	Average DEC Error (Degrees)	# of Obs
December 8, 2022	Earth Return	15.30	0.0017	0.0021	88
December 9, 2022	Earth Return	14.81	0.0039	0.0009	59

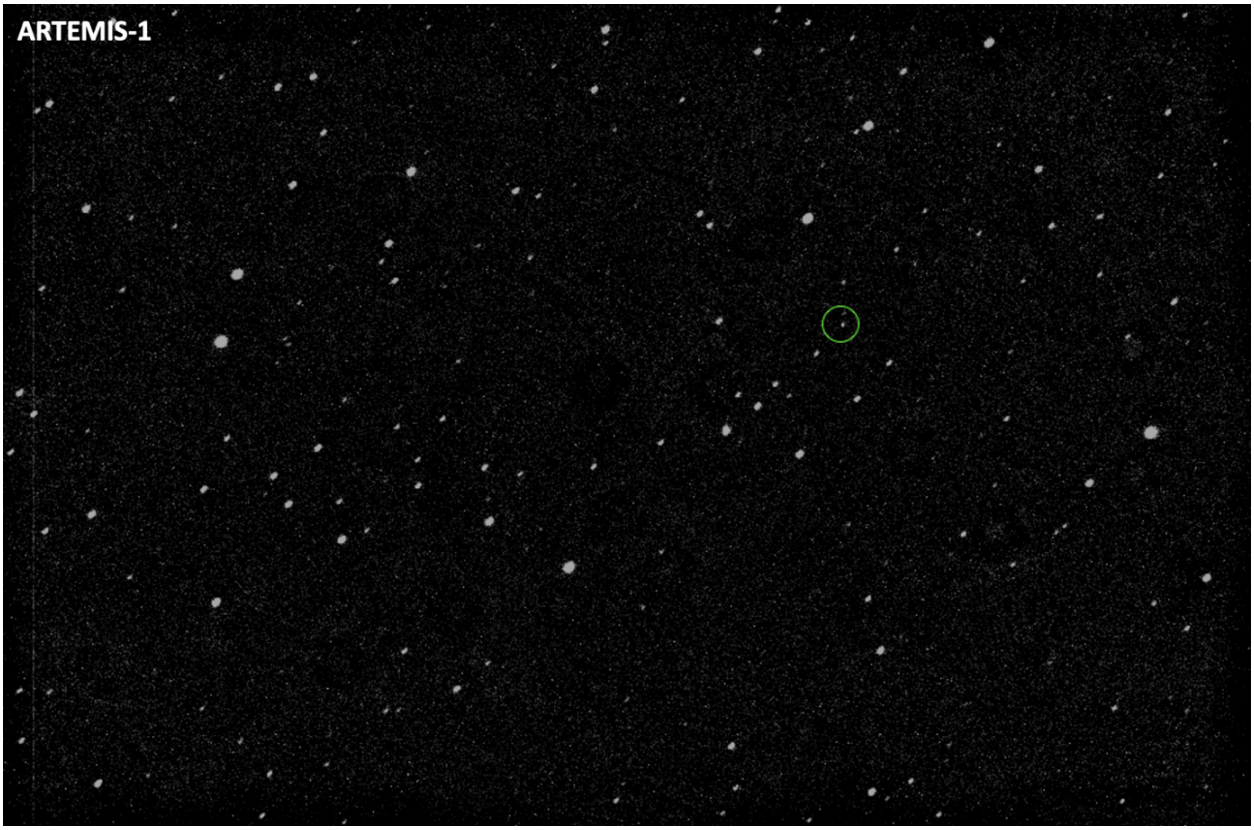

Fig. 6: Imagery of the Orion spacecraft taken with the MITRE Observatory on December 9, 2022, while the spacecraft was returning from lunar orbit.

The Orion spacecraft served as a moving cislunar object test case. Orion was best imaged using rate tracking due to the increased angular rates of the traveling spacecraft. For imaging, we found using a 30-second exposure most successful between collecting enough signal on the target without external disturbances affecting the images. Shorter image spacing of 10 minutes was successful in allowing for visible changes in position of the target within imagery while a 30-minute total collection window was used. The astrometric errors for RA and DEC are inline with the JWST results which matches our expectations.

GEOTAIL (SATID 22049)

GEOTAIL was observed while in orbit around the Earth up to 200,000 kilometers away. GEOTAIL is an example of an object whose orbit extends beyond GEO but is not traveling within the vicinity of the Moon. Table 4 summarizes the observation results for the GEOTAIL satellite while Fig. 7. shows example imagery of the spacecraft.

Table 4: Observation results for the GEOTAIL survey satellite.

Date	Mission Stage	Average Visual Magnitude	Average RA Error (Degrees)	Average DEC Error (Degrees)	# of Obs
December 1, 2022	Orbit	8.3276	0.0156	0.0300	15
February 2, 2023	Orbit	9.4677	0.0175	0.0173	40
February 7, 2023	Orbit	10.562	0.0110	0.0134	20
April 11, 2023	Orbit	12.179	0.0160	0.0096	38

GEOTAIL is a small satellite (2.2m x 1.6m) at large distances from Earth making it a difficult target to track [14]. It was best imaged using rate tracking due to the increased angular rate of the orbiting satellite. For imaging, we found increased exposure times up to 120 seconds the most successful for collecting enough signal on the small target. The extended exposure times made collecting imagery of the satellite more difficult as we were more prone to external disturbances from the environment. Shorter image spacing of 10 minutes was successful in allowing visible changes in the targets position with 30 minutes total being a sufficient collection window.

For the astrometric errors presented in the observation results tables, we use ephemeris generated from the JPL Horizons Service as the truth data compared to our observation measurements. Using the image timestamps as our ephemeris epoch, we produced state vector information on Horizons for each image to use in the calculations. The errors listed in the tables are the result of taking the difference between the Horizons RA and DEC values and our observation measurements for all images on a given night. All targets, regardless of being in transit during a mission or in orbit, produced consistent and similar errors throughout the collection campaign with an average RA error of 0.0080 degrees and an average DEC error of 0.0057. For LEO/GEO observations using the same telescope hardware and image processing software, the RA errors are on average 0.0006 degrees while DEC errors are on average 0.0005 degrees. The XGEO observation errors are approximately 10x larger than the LEO/GEO observation residuals. While these errors may seem alarming, there are additional processing steps such as light time correction that are not applied that would potentially decrease these errors.

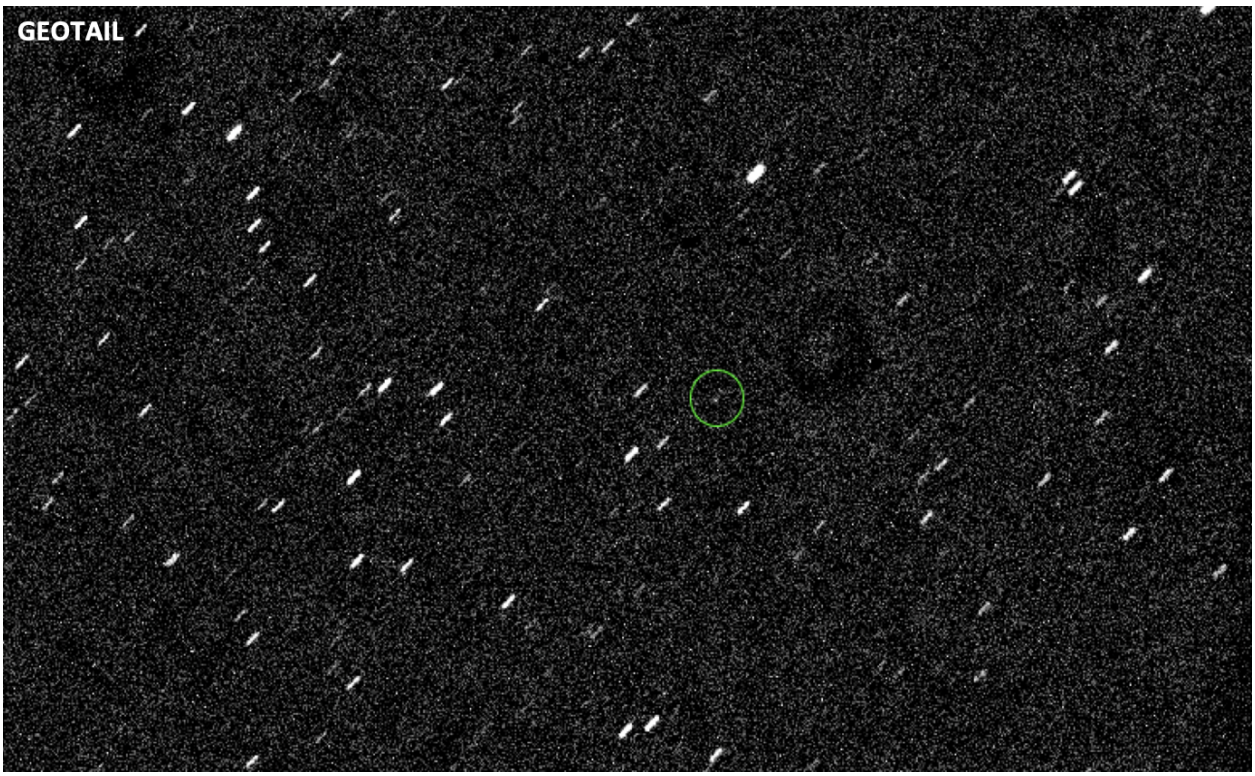

Fig. 7: Imagery of the GEOTAIL satellite taken with the MITRE Observatory on February 2, 2023.

5. SUMMARY

This research began with the launch of the James Webb Space Telescope in December of 2021 after realizing that the typical techniques used for LEO/GEO observations are rendered unusable for spacecraft in XGEO space. As humans begin their return to the lunar surface and as more missions are planned for beyond GEO, the necessity to understand this area of space and to develop a ground-based optical observing procedure increases. The purpose of our work is to not only develop an observing procedure but to provide solutions to the discussed sensing and astrodynamics challenges. This report provides details on the final observation procedure that MITRE has created to handle XGEO observations, which has been successful in producing imagery and metric observation data on spacecraft such as the James Webb Space Telescope, the Orion Spacecraft from the Artemis-1 Mission, and more. Aside from the observation procedure, we have created a novel data set of XGEO observations within the UDL for industry usage.

We intend to continue adding to this data set and to further develop the observing procedure as more difficult objects and missions are deployed beyond GEO. This work allows us to provide consistent imagery and metric observations for XGEO objects, something that was previously unavailable, and increases our understanding of this new region of space that is quickly being proliferated. This research is funded by MITRE's Independent Research and Development Program.

REFERENCES

[1] B Dunbar. *Commercial Lunar Payload Services Overview*. https://www.nasa.gov/commercial-lunar-payload-services-overview. 2019.

[2] NASA. *NASA Space Science Data Coordinated Archive Luna 25 Spacecraft Details*. https://nssdc.gsfc.nasa.gov/nmc/spacecraft/display.action?id=LUNA-25. 2022.

[3] NASA. *NASA Space Science Data Coordinated Archive Smart Lander for Investigating Moon Spacecraft Details*. https://nssdc.gsfc.nasa.gov/nmc/spacecraft/display.action?id=SLIM. 2022.

[4] M. J. Holzinger, C. C. Chow P Garretson. "A Primer on Cislunar Space". In: (2021).

[5] NASA. *What is a Lagrange Point?* https://solarsystem.nasa.gov/resources/754/what-is-a-lagrange-point/. 2018.

[6] NASA. *Three-Body Periodic Orbits*. https://ssd.jpl.nasa.gov/tools/periodic_orbits.html.

[7] K. Raub, T. McLaughlin R. Mansfield. "XGEO Collection Methods Using New Satellite Observing Techniques on the James Webb Space Telescope". In: *AMOS Technical Paper Library* (2022).

[8] NASA. *Webb Key Facts*. https://webb.nasa.gov/content/about/faqs/facts.html.

[9] NASA. *Webb Orbit*. https://webb.nasa.gov/content/about/orbit.html. 2022.

[10] P. Sabelhaus J. Decker. *An Overview of the James Webb Space Telescope (JWST) Project*. https://doi.org/10.1117/12.549895. 2004.

[11] NASA. *NASA's Lunar Exploration Program Overview*. https://www.nasa.gov/sites/default/files/atoms/files/artemis_plan-20200921.pdf. 2020.

[12] NASA. *NASA Artemis*. https://www.nasa.gov/specials/artemis/. 2019.

[13] NASA. *GEOTAIL - NASA Solar System Exploration*. https://solarsystem.nasa.gov/missions/geotail/in-depth/. 2023.

[14] Institute of Space and Astronautical Science. *GEOTAIL Spacecraft*. https://www.isas.jaxa.jp/en/missions/spacecraft/past/geotail.html.

[15] NASA. *Horizons System*. https://ssd.jpl.nasa.gov/horizons/app.html.

[16] D. Cicco. *Hunting Asteroids From Your Backyard*. https://skyandtelescope.org/observing/hunting-asteroids-from-your-backyard/. 2006.